Processing of the VP1/2A Junction Is Not Necessary for Production of Foot-and-Mouth Disease Virus Empty Capsids and Infectious Viruses: Characterization of "Self-Tagged" Particles

Gullberg, Maria; Polacek, Charlotta; Bøtner, Anette; Belsham, Graham

Published in:
Journal of Virology

Link to article, DOI:
10.1128/JVI.01863-13

Publication date:
2013

Document Version
Publisher's PDF, also known as Version of record

Journal of Virology

Processing of the VP1/2A Junction Is Not Necessary for Production of Foot-and-Mouth Disease Virus Empty Capsids and Infectious Viruses: Characterization of "Self-Tagged" Particles

Maria Gullberg, Charlotta Polacek, Anette Bøtner and Graham J. Belsham

J. Virol. **2013, 87(21):11591. DOI: 10.1128/JVI.01863-13.**
Published Ahead of Print 21 August 2013.

JVI Journals.ASM.org

Processing of the VP1/2A Junction Is Not Necessary for Production of Foot-and-Mouth Disease Virus Empty Capsids and Infectious Viruses: Characterization of "Self-Tagged" Particles

Maria Gullberg, Charlotta Polacek, Anette Bøtner, Graham J. Belsham

National Veterinary Institute, Technical University of Denmark, Lindholm, Kalvehave, Denmark

The foot-and-mouth disease virus (FMDV) capsid protein precursor, P1-2A, is cleaved by $3C^{pro}$ to generate VP0, VP3, VP1, and the peptide 2A. The capsid proteins self-assemble into empty capsid particles or viruses which do not contain 2A. In a cell culture-adapted strain of FMDV (O1 Manisa [Lindholm]), three different amino acid substitutions (E83K, S134C, and K210E) were identified within the VP1 region of the P1-2A precursor compared to the field strain (wild type [wt]). Expression of the O1 Manisa P1-2A (wt or with the S134C substitution in VP1) plus $3C^{pro}$, using a transient expression system, resulted in efficient capsid protein production and self-assembly of empty capsid particles. Removal of the 2A peptide from the capsid protein precursor had no effect on capsid protein processing or particle assembly. However, modification of E83K alone abrogated particle assembly with no apparent effect on protein processing. Interestingly, the K210E substitution, close to the VP1/2A junction, completely blocked processing by $3C^{pro}$ at this cleavage site, but efficient assembly of "self-tagged" empty capsid particles, containing the uncleaved VP1-2A, was observed. These self-tagged particles behaved like the unmodified empty capsids in antigen enzyme-linked immunosorbent assays and integrin receptor binding assays. Furthermore, mutant viruses with uncleaved VP1-2A could be rescued in cells from full-length FMDV RNA transcripts encoding the K210E substitution in VP1. Thus, cleavage of the VP1/2A junction is not essential for virus viability. The production of such engineered self-tagged empty capsid particles may facilitate their purification for use as diagnostic reagents and vaccines.

Foot-and-mouth disease virus (FMDV), the prototype member of the *Aphthovirus* genus within the family *Picornaviridae*, is a highly contagious agent infecting cloven-hoofed animals (including cattle, pigs, sheep, and goats), and it causes one of the most economically important animal diseases worldwide (1).

Each FMDV particle contains a single-stranded positive-sense RNA genome (ca. 8,400 nucleotides [nt]) enclosed by an icosahedral protein shell (capsid) consisting of 60 copies of each of the four structural proteins VP1, VP2, VP3, and VP4 (2). The surface-exposed FMDV capsid proteins (all but VP4, which is entirely internal) play a key role in the antigenic properties of the virus (e.g., defining the serotype). In addition, the capsid surface has to interact with various cell surface receptor molecules, such as integrins and heparan sulfate glycosaminoglycans (for some tissue culture-adapted variants) (3), prior to cell entry by clathrin- or caveola-mediated endocytosis (4–8). Following virus entry, the acidic pH within endosomes triggers capsid disassembly, allowing release of the viral RNA genome into the cytoplasm of the cells where replication occurs.

Picornavirus genomes contain a single, long open reading frame (ORF; ca. 7,000 nt for FMDV) encoding a polyprotein which is rapidly processed by virus-encoded proteases. The overall organization of the viral polyproteins, with three or four primary precursor proteins, i.e., a leader (L) protein (in most cases), the structural proteins (P1 and P1-2A), and nonstructural proteins (P2 and P3), is shared among different picornaviruses. However, the sequences flanking the structural protein precursor (at both the N terminus and C terminus) can be quite diverse between different members of this virus family. Most picornaviruses (except the enteroviruses, e.g., poliovirus) contain an L protein at the N terminus of the polyprotein, but the functions of these L proteins vary. In the case of the aphthoviruses and the erboviruses, the L protein is a papain-like cysteine protease which cleaves the L/P1 junction (9–11).

On the C-terminal side of the P1 sequence, the enterovirus 2A protein is a chymotrypsin-like protease which catalyzes the cleavage of the junction between the P1 and P2 precursor (at the VP1/2A junction) within the polyprotein and also induces the inhibition of host cell protein synthesis (12, 13). In the case of the aphtho- and cardioviruses (e.g., encephalomyocarditis virus [EMCV]), the capsid protein precursor is P1-2A, and a primary polyprotein cleavage occurs at the 2A/2B junction within a conserved DvExNPG/P motif. These 2A proteins lack characteristic protease motifs, and the break in the polyprotein chain, dependent on the 2A sequence, occurs cotranslationally; it may be that the polypeptide bond between the G and P residues is never made as a result of ribosome skipping (2, 14). A third type of 2A protein is encoded by the genome of hepatitis A virus (HAV; within the *Hepatovirus* genus). The HAV 2A protein plays an important role in the virion assembly process, although after assembly it is cleaved away from the VP1-2A intermediate and is absent from the mature particle (15–19).

The 2A peptide of FMDV is only 18 amino acids in length, and it shows a high degree of amino acid similarity to the C terminus of the much larger cardiovirus 2A proteins (14, 20). As indicated above, in contrast to the P1 capsid precursor of enteroviruses, the

Received 8 July 2013 **Accepted** 14 August 2013
Published ahead of print 21 August 2013
Address correspondence to Graham J. Belsham, grbe@vet.dtu.dk.

doi:10.1128/JVI.01863-13

capsid precursor of FMDV includes the 2A protein; therefore, it is called P1-2A. $3C^{pro}$ is responsible for processing of the FMDV P1-2A precursor into VP0, VP3, and VP1 plus 2A. There is evidence that cleavage of the VP1/2A junction is relatively slow compared to that of the other sites within P1-2A that are cleaved by $3C^{pro}$ (21, 22), since VP1-2A can still be readily detected after complete loss of the intact P1-2A and maximal formation of VP0. The processed capsid proteins remain associated with each other (within a protomer) and can associate into pentamers, and then 12 of these can self-assemble into empty capsids. Formation of mature virus particles requires encapsidation of the viral genome. During the assembly process, cleavage of VP0 to VP4 and VP2 occurs through an unknown mechanism. It has usually been considered that the encapsidation of the RNA is the trigger for VP0 cleavage, but several studies have shown that VP0 cleavage occurs within assembled empty capsids as well (22–24). The function (if any) of the FMDV 2A within the P1-2A capsid precursor and during assembly of the capsid proteins is unknown, but a previous study (25) has indicated that the presence of 2A is not required for assembly of FMDV pentamers *in vitro*.

In the enteroviruses and cardioviruses, most of the $3C^{pro}$ cleavage sites are at glutamine (Gln [Q])/glycine (Gly [G]) amino acid pairs. The FMDV $3C^{pro}$-mediated processing at the various cleavage sites shows greater, but still limited, diversity in the recognition sequence, and the sequences have either glutamine (Gln [Q]) or glutamate (Glu [E]) at the P1 position (i.e., P1-Gln or P1-Glu) of the bond to be cleaved (26). The VP1/2A junction for serotype O and A FMDVs is generally PxKQ/xLNF; thus, it has a Gln residue at the P1 position, which, together with the P4-Pro (P), P2-Lys (K), and P4′-Phe (F) residues, represent the most important determinants of $3C^{pro}$ specificity at this site (26–28). Studies of aligned FMDV $3C^{pro}$ cleavage sequences for over 100 strains of the virus (including representatives of all seven serotypes) reveal that sites with P1-Gln have a strong selectivity for P2-Lys, which suggests that recognition of the P1 residue by $3C^{pro}$ is influenced by the residue in position P2 (26).

Several studies have investigated processing of the FMDV P1-2A precursor by $3C^{pro}$ (for examples, see references 21, 29, and 30). Previous reports from our laboratory have described the expression and properties of P1-2A (both for FMDV serotype O and A) in the presence of $3C^{pro}$ (22, 31). Using transient expression assays, the processed FMDV capsid proteins were efficiently and appropriately produced in BHK cells; the products assembled into empty capsid particles that could be isolated using sucrose gradient centrifugation (22). These particles had the ability to bind to both the FMDV receptor $\alpha_v\beta_6$ integrin and appropriately to serotype-specific anti-FMDV antibodies. We now describe experiments designed to examine the role of the FMDV 2A peptide in capsid assembly. Neither blocking the removal of the 2A peptide from the VP1-2A precursor nor deleting 2A entirely resulted in any apparent effect on empty capsid particle assembly. Thus, the formation of empty capsid particles containing VP1-2A together with VP0 and VP3 provided the first evidence for the formation of "self-tagged" FMDV empty capsids. Furthermore, it is also shown that FMDVs with an uncleavable VP1/2A junction can be produced which are infectious in cell culture.

MATERIALS AND METHODS

Viral RNA extraction, cDNA synthesis, PCR, and sequencing. The FMDV O1 Manisa strain (originally isolated in Turkey in 1969) was obtained in 1994 from The Pirbright Institute (Institute for Animal Health, United Kingdom) after 7 passages in baby hamster kidney (BHK) cells and then propagated four times in primary bovine kidney cells (referred to as O1 Manisa [Lindholm] in this paper). Viral RNA was extracted from infected cell cultures (QIAamp viral RNA minikit; Qiagen) and reverse transcribed using Ready-To-Go you-prime first-strand beads (GE Healthcare Life Sciences). cDNA corresponding to the capsid coding region was amplified in a PCR (Expand high-fidelity PCR system; Roche) using virus-specific primers (Table 1). The amplicons covering the entire P1-2A coding region were visualized in agarose gels and purified (GeneJET gel extraction kit; Fermentas). The products were sequenced on both strands with an ABI Genetic Analyzer 3500 (Applied Biosystems) using BigDye chemistry (ABI Prism BigDye Terminator cycle sequencing ready reaction kit, version 1.1; Applied Biosystems). Sequences were analyzed using Vector NTI software (Invitrogen).

TABLE 1 Primers

Primer name[a]	Sequence[b] (5′–3′)
1-O PN 3 Fw*	AACCACTCAACGGAGAGTGGAA
1-V PN 48 Re*	ACTGTACTGTGYRWAGTACTGGGC
8-A PN 51 Fw*	CCACAGATCAAGGTGTATGC
1-O PN 20 Re*	GACATGTCCTCCTGCATCTG
FMDVOP1_*Asc*I*Xma*I_Re	CTACCCGGGGGCGCGCCTGGGCCCAGGGTTGG ACTCCACATCTC
FMDVAP1_*Asc*I*Bam*HI_Re	CTAGGATCCGGCGCGCCTGGGCCCGGGGTTGG ACTCAACGTCTCCT
FMDVA_VP1K210E_Fw	CCTGCA**G**AACAACTTTTGAACTTCGATTTGCT CAAGTTG
FMDVA_VP1K210E_Re	AAGTTGTT**C**TGCAGGTGCAATGATCTTCTGTT TGTGTCT
FMDVO_VP1E83K_Fw	AAGCAC**A**AGGGAAACCTCACCTGGGTCCCGA ACGGGGCG
FMDVO_VP1E83K_Re	GTTTCCCT**T**GTGCTTCACTGCCACCTCTAAGT CAGCGAA
FMDVO_VP1C134S_Fw	GGGAAC**A**GCAAGTATGGTGACGGCACGGTG GCCAATGTG
FMDVO_VP1C134S_Re	ATACTTGC**T**GTTCCCGTTGTAAACAGTAGCC AACACGCG
FMDVO_*Nhe*IVP4VP2_Fw	CGCTCTGCTAGCCGACAAGAAAACCGAGGAGACC
FMDVO_*Apa*I2A2B_Re	CTACTAGGGCCCAGGGTTGGACTCCACATCTCCC

[a] Asterisks indicate primers used to amplify parts of the P1-2A coding region of FMDV O1 Manisa (Lindholm).
[b] Underlined sequences represent restriction enzyme sites AscI, BamHI, XmaI, NheI, and ApaI. Nucleotide changes producing amino acid substitutions are shown in boldface.

Construction of FMDV capsid cDNA expression cassettes. The FMDV cDNA cassettes used in this study are shown in Fig. 1 and were prepared by standard methods (32). pGEM-3Z-P1-2A (31), as well as its derivatives pGEM-3Z-P1-2A-3Cwt, pGEM-3Z-P1-2A-3CC142S, and pGEM-3Z-P1-2A-IRESgtta3Cwt (22), for both FMDV serotype O and serotype A have been described elsewhere. For simplicity, the pGEM-3Z-P1-2A-IRESgtta3Cwt plasmid is referred to here as pGEM-3Z-P1-2A-mIRES-3C (Fig. 1).

The cDNAs for the P1 (lacking 2A) coding regions were amplified using FMDV serotype O and serotype A primers (FMDVO_*Eco*RI_Fw, FMDVOP1_*Asc*I*Xma*I_Re, FMDVA_*Eco*RI_Fw, and FMDVAP1_*Asc*I*Bam*HI_Re) (31 and Table 1), which included EcoRI and AscI-XmaI or AscI-BamHI restriction enzyme sites, respectively. These PCR products (~2,300 bp) were digested with EcoRI and XmaI or BamHI, respectively, and inserted into the same sites of pGEM-3Z (Promega), generating pGEM-3Z-O-P1 and pGEM-3Z-A-P1. The cDNA fragments, including 3Cwt, 3CC142S, and mIRES-3C, were introduced as described previously (22) to produce the expression plasmids pGEM-3Z-P1-3Cwt, pGEM-3Z-P1-3CC142S, and pGEM-3Z-P1-mIRES-3C.

The cDNA for the whole P1-2A region from FMDV O1 Manisa (Lindholm) cDNA was amplified using primers FMDVO_*Eco*RI_Fw and FMDVO_*Asc*I*Xma*I_Re (31), and a pGEM-3Z-O-P1-2ALindholm-mIRES-3C vector was constructed as described above. The O1 Manisa sequence used as the wild-type (wt) sequence encodes residue 134 of VP1

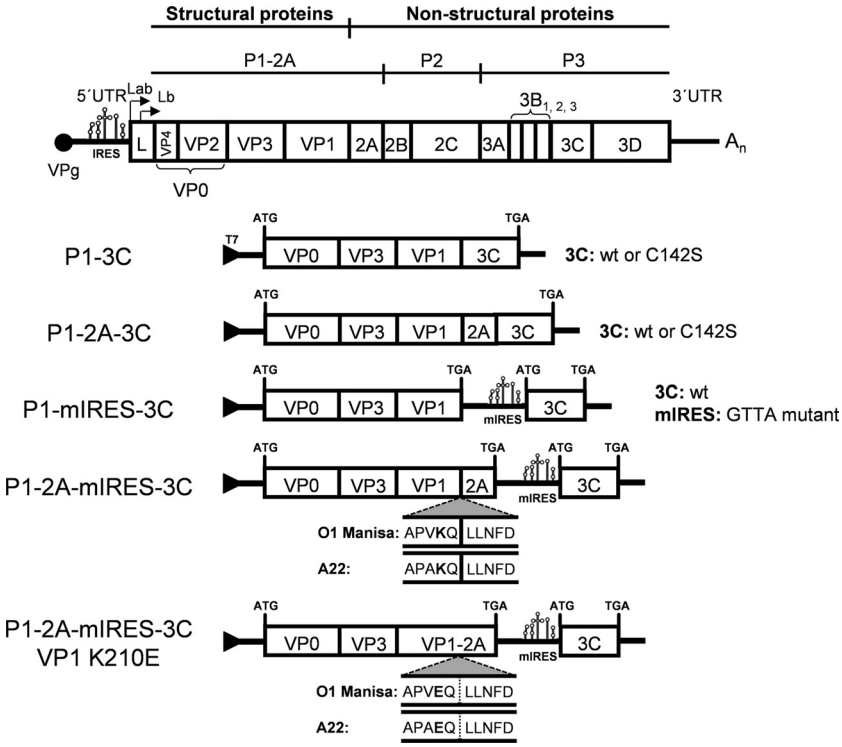

FIG 1 Schematic representation of the FMDV genome organization and cDNA expression cassettes for FMDV capsid proteins. Plasmids are based on pGEM-3Z and possess an ampicillin cassette for selection. The P1-2A, P1-2A-3C, and P1-2A-mIRES-3C FMDV cDNA cassettes have been described elsewhere (22, 31). P1 and P1-2A, capsid precursor proteins; 3C, $3C^{pro}$ wt or C142S; mIRES, internal ribosome entry site with the GTTA mutant motif; VP1 K210E, VP1/2A cleavage site mutant; ATG, start codon; TGA, stop codon; UTR, untranslated region. The two forms of the L protein, termed Lab and Lb, are made by translation initiation at separate AUG codons 84 nt apart.

as a Cys (C) rather than the Ser (S) present in the field strain (GenBank accession no. AY593823). The resulting plasmid, containing the O1 Manisa (Lindholm) cDNA sequence, was then digested with AgeI and SacI, and the ~600-bp fragment was used to replace the corresponding fragment of pGEM-3Z-O-P1-2A-mIRES-3C to generate pGEM-3Z-O-P1-2A-mIRES-3C VP1K210E. The QuikChange site-directed mutagenesis method (with PfuTurbo DNA polymerase; Stratagene) was used, according to the manufacturer's instructions, with primers containing the desired mutations (Table 1) to produce the following plasmids with the indicated substitutions: pGEM-3Z-A-P1-2A-mIRES-3C VP1K210E, pGEM-3Z-O-P1-2A-mIRES-3C VP1E83K, pGEM-3Z-O-P1-2A-mIRES-3C VP1C134S, and the double mutant pGEM-3Z-O-P1-2A-mIRES-3C VP1E83K and VP1K210E. All plasmids were propagated in *Escherichia coli* Top10 cells (Invitrogen), purified (Midiprep kit; Fermentas), and verified by sequencing.

Transient expression assays. BHK cells (35-mm wells, ca. 90% confluent) were infected with a recombinant vaccinia virus (vTF7-3) that expresses the bacteriophage T7 RNA polymerase (33) as described previously (34). After virus adsorption for 1 h at 37°C, the infected cells were transfected with 2 μg of the indicated plasmid DNA using FuGENE 6 (Promega) as described by the manufacturer. At 20 h posttransfection, cell lysates were prepared using 20 mM Tris-HCl (pH 8.0), 125 mM NaCl, and 0.5% NP-40 and clarified by centrifugation at 18,000 × *g* for 10 min at 4°C.

Immunoblot analysis. Immunoblotting was performed according to standard methods as described previously (31). Briefly, samples were mixed with Laemmli sample buffer, separated by SDS-PAGE (12.5% polyacrylamide), and transferred to polyvinylidene difluoride (PVDF) membranes (Millipore). After blocking in 5% nonfat dry milk and 0.1% Tween 20 in phosphate-buffered saline (PBS), membranes were incubated with primary antibodies diluted in the same buffer. The following primary antibodies were used: anti-FMDV O1 Manisa serum (which recognizes the capsid proteins), serotype-independent anti-FMDV VP2 4B2 (kindly provided by L. Yu, Harbin, China [35]), anti-2A (ABS31; Millipore), and anti-actin (ab8227; Abcam). Immunoreactive proteins were visualized using appropriate secondary horseradish peroxidase-conjugated antibodies (Dako) and a chemiluminescence detection kit (ECL Prime; Amersham) with a Chemi-Doc XRS system (Bio-Rad).

Antigen ELISAs. Serotype-specific FMDV antigen enzyme-linked immunosorbent assays (ELISAs), for serotype O and A as appropriate, were performed as described previously (31, 36, 37). Briefly, plates were coated with serotype-specific rabbit anti-FMDV antisera, and the FMDV antigen was captured from the samples and then detected using guinea pig anti-FMDV antisera plus horseradish peroxidase-conjugated anti-guinea pig antibodies.

The ELISA to detect the presence of the FMDV 2A peptide (while fused to P1 or VP1) was performed similarly but with the following differences. The plates were coated with a serotype-specific guinea pig anti-FMDV polyclonal antibody as the capture reagent. After blocking with wash buffer containing 2% bovine serum albumin, the test samples were added. Detection of the bound FMDV 2A peptide (e.g., as VP1-2A or P1-2A) was achieved using rabbit anti-2A antibodies (ABS31; Millipore) diluted in binding buffer and secondary horseradish peroxidase-conjugated anti-rabbit antibodies (Dako) diluted in binding buffer containing 5% guinea pig serum.

The ELISA to detect FMDV antigen binding to the human integrin receptor $\alpha_v\beta_6$ (38) was performed as described previously (31). Briefly, plates were coated with purified recombinant human $\alpha_v\beta_6$ integrin (0.5 μg/ml; R&D Systems), the test samples were added, and the bound FMDV antigen was detected using polyclonal guinea pig anti-FMDV antibody plus rabbit anti-guinea pig Ig conjugated to horseradish peroxidase (Dako).

Sucrose gradient analysis. Cell extracts from transfected cells (400 μl of lysate from one 35-mm well per gradient) were loaded onto 10 to 30% (wt/vol) sucrose gradients in 40 mM sodium phosphate buffer (pH 7.6) with 100 mM NaCl (buffer P) and centrifuged at 245,000 × *g* in an SW 55 Ti rotor (Beckman Coulter) for 2.5 h at 10°C. Fractions were collected from the top of the gradient, and viral proteins were detected by the serotype-specific FMDV antigen ELISA, FMDV 2A-specific ELISA (as described above), and immunoblotting (as described above).

Modification of full-length FMDV cDNAs. Plasmids containing the FMDV O1Kaufbeuren (O1K) cDNA have been described previously (39, 40). The cDNA corresponding to the O1 Manisa VP2-2A coding region was amplified from pGEM-3Z-O-P1-2A (31) and pGEM-3Z-O-P1-2A-mIRES-3C VP1K210E (described above) using primers FMDVO_*Nhe*IVP4VP2_Fw and FMDVO_*Apa*I2A2B_Re (Table 1). The introduction of the NheI and ApaI restriction enzyme sites in the PCR primers did not cause amino acid changes in the sequence. The VP2-2A amplicons (~2,000 bp) were digested with NheI and ApaI and inserted into a similarly digested intermediate plasmid containing the ca. 5-kbp XbaI fragment from pT7S3 (39) essentially as described previously (40). The VP3 coding region of FMDV O1 Manisa includes an NheI site; thus, this insertion was performed in two steps. These plasmids were digested with XbaI, and the fragments were ligated into the XbaI-digested backbone of pT7S3 (39) to generate pO1K/O1Manisa wt and pO1K/O1Manisa VP1K210E containing full-length FMDV cDNAs. The plasmids were propagated in *E. coli*, purified, and verified by sequencing as described above.

Rescue of viruses from full-length FMDV cDNA. The plasmids pO1K/O1Manisa wt and pO1K/O1Manisa VP1K210E were linearized by digestion with HpaI, purified (QIAquick PCR purification kit; Qiagen), and *in vitro* transcribed using T7 RNA polymerase (Megascript kit; Ambion) as described by the manufacturer. The RNAs were analyzed using agarose gel electrophoresis and then introduced into BHK cells by electroporation as described previously (40, 41). At 2 to 3 days postelectroporation, the viruses were harvested and amplified in one or two subsequent passages (P2 or P3) in BHK cells. After these passages, viral RNA was extracted, reverse transcribed, PCR amplified, and sequenced as described above. Note that control reaction mixtures lacking reverse transcriptase were used to show that the PCR products obtained were derived from the viral RNA template. Viral titers were determined, as 50% tissue culture infectious doses ($TCID_{50}$), by titration in BHK cells according to standard procedures (42).

Immunofluorescence assays. Monolayers of BHK cells grown on glass coverslips in 35-mm-well plates were infected with O1K/O1 Manisa wt or VP1 K210E mutant at a multiplicity of infection (MOI) of 0.1 $TCID_{50}$/cell. After 4 h, the cells were fixed by incubation in 4% paraformaldehyde (in PBS) for 10 min at room temperature, followed by incubation in methanol for 10 min at −20°C. The coverslips were washed three times in PBS before incubation with blocking buffer (5% horse serum in PBS) for 1 h at room temperature. The cells were stained with a primary polyclonal rabbit anti-FMDV O1 Manisa antibody or rabbit anti-2A (ABS31; Millipore), diluted in blocking buffer, for 2 h at room temperature. Washed coverslips were then incubated with a donkey anti-rabbit antibody labeled with Alexa Fluor 568 (A10042; Life Technologies) in blocking buffer for 1 h at room temperature. The slides were mounted with Vectashield (Vector Labs) containing 4′,6-diamidino-2-phenylindole (DAPI), and images were captured using an epifluorescence microscope.

Immunoblot analysis of FMDV-infected cells. Monolayers of BHK cells, grown in 35-mm wells, were inoculated with the rescued chimeric viruses (O1K/O1 Manisa wt and O1K/O1 Manisa VP1K210E) at an MOI of 0.1 $TCID_{50}$/cell. Cell lysates were prepared at 2, 4, and 6 h postinfection and analyzed by immunoblotting using anti-2A antibodies as described above.

TABLE 2 Predicted amino acid differences between the field FMDV O1 Manisa sequence and FMDV O1 Manisa (Lindholm)[a]

VP1 residue	Amino acid		Comment(s)
	O1 Manisa	O1 Manisa (Lindholm)	
83	E	K	Surface exposed on capsid, close to the 5-fold axis; E83 is conserved (in FMDV serotype O)
134	S	C	Surface exposed on capsid (GH loop)
210	K	E	At the VP1/2A cleavage site (P2 position); K210 is conserved (in FMDV serotype O)

[a] The sequence of the FMDV O1 Manisa strain is registered under GenBank accession number AY593823.

RESULTS

Amino acid variation within the FMDV O1 Manisa P1-2A capsid precursor. Comparison of the published FMDV O1 Manisa (GenBank accession number AY593823) P1-2A capsid coding sequence to that of the O1 Manisa (Lindholm) isolate predicted three amino acid substitutions within the entire P1-2A capsid precursor, each within VP1. The changes are E83K, S134C, and K210E. The predicted amino acid substitutions and their locations are summarized in Table 2. Residue E83 of VP1 is predicted to be exposed on the virion surface in the loop connecting the βD and βE strands (43, 44) and has been associated with cell culture adaptation in both serotype O and SAT2 viruses (44, 45). The residue 134 (Ser [S]) is located at the base of the loop connecting βG2 and βH strands of the VP1 protein (known as the GH loop) (43, 46). This loop is surface exposed and contains a major antigenic site plus the RGD motif (residues 145 to 147), which is critical for the integrin receptor recognition. Residue 210 (Lys [K]) is located close to the C terminus of VP1, i.e., at position P2 within the VP1/2A cleavage site (KQ/LL). Based on a sequence alignment and comparison of the VP1/2A junctions from over 100 strains of FMDV (26, 47), it is apparent that the P2-Lys residue is highly conserved among FMDV strains. Among the 100 strains compared previously (47), P2-Lys was present in 96 strains, while P2-Arg (another positively charged residue) was present in 4 serotype A viruses. Thus, the K210E change, which introduces a negatively charged amino acid (Glu [E]) in place of a positively charged amino acid (Lys [K]) at the P2 position in the VP1/2A cleavage site, had unknown consequences for protein processing.

3C^{pro} processing of the VP1/2A cleavage site. To examine the cleavage of the FMDV VP1/2A junction by 3C^{pro}, the O1 Manisa P1-2A precursor, either wt or with the VP1 K210E substitution, was expressed within BHK cells in the presence of the FMDV 3C^{pro}. Since high-level 3C^{pro} expression diminishes the yield of expressed FMDV capsid proteins in this system (31), previously described P1-2A-3Cwt, P1-2A-3CC142S, and P1-2A-IRESgtta-3Cwt (here referred to as P1-2A-mIRES-3C) cDNA cassettes (Fig. 1) were used which express different levels of 3C^{pro} activity (22, 31). In addition, the corresponding cassettes containing P1 (rather than P1-2A) were used to provide markers for the FMDV proteins lacking the 2A peptide. The expression and processing of the products generated from these plasmids was visualized in im-

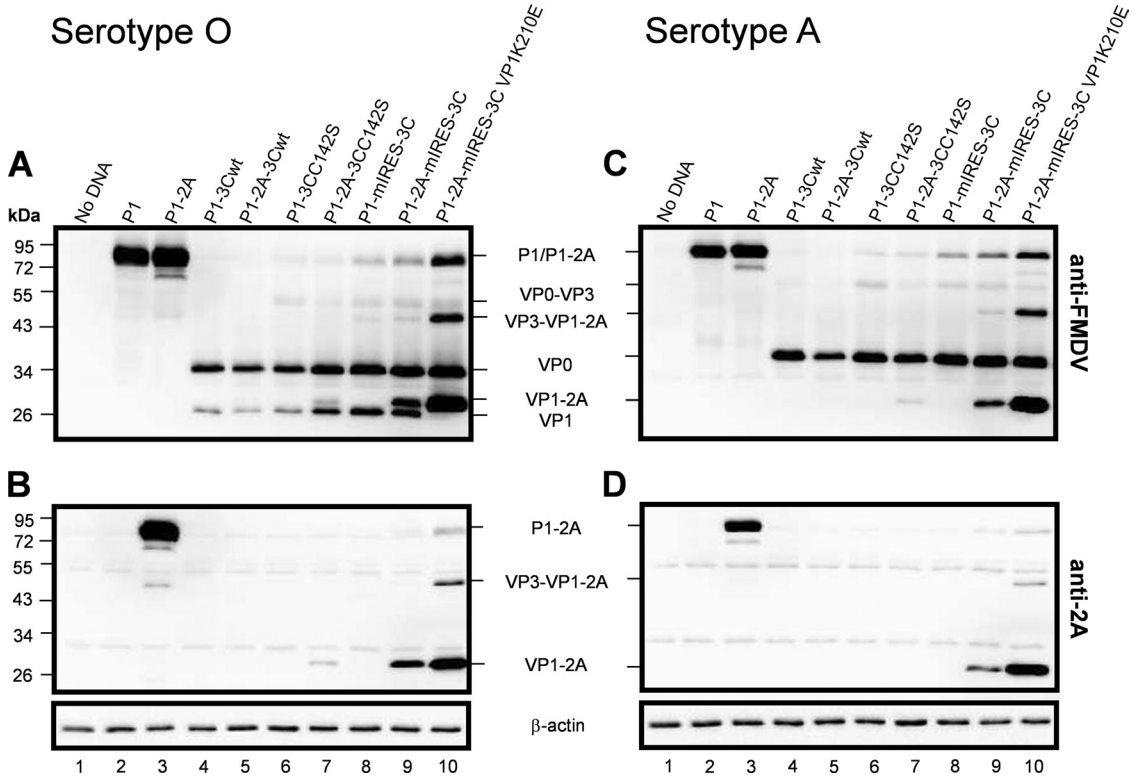

FIG 2 Expression and $3C^{pro}$ processing of FMDV capsid protein precursor P1, P1-2A, or P1-2A (VP1 K210E). Plasmids containing the FMDV serotype O (A and B) or serotype A (C and D) cDNA cassettes were transfected into BHK cells infected with recombinant vaccinia virus vTF7-3. Cytoplasmic extracts were prepared 20 h posttransfection and fractionated by SDS-PAGE, followed by transfer to PVDF membrane and probing with antibodies specific for FMDV capsid proteins (A and C), FMDV 2A protein (B and D), and β-actin (bottom panels). Expression of β-actin was used as a control of equal protein loading. The results shown are representative of two independent experiments. Molecular mass markers (kDa) are indicated in the left margin.

munoblots using antibodies directed against the FMDV capsid proteins and against the 2A peptide. Expression of serotype O P1 or P1-2A cDNA cassettes alone led to P1 and P1-2A products of the expected molecular masses (approximately 85 kDa) (Fig. 2A, lanes 2 and 3). Note that the small difference in expected size (ca. 2 kDa), due to the presence of the 2A peptide, cannot be detected within the context of this large molecule. In the presence of $3C^{pro}$, both P1 and P1-2A were efficiently processed (Fig. 2A, lanes 4 to 9). The products derived from P1-2A were identified as VP0 (approximately 36 kDa), VP1 (approximately 28 kDa), and VP1-2A (approximately 30 kDa) (Fig. 2A, lane 9) on the basis of their calculated molecular masses (33, 23, and 25 kDa, respectively). These two forms of VP1 indicate incomplete processing at the VP1/2A junction, i.e., the presence of both the mature VP1 protein and the VP1-2A precursor. The specific antiserum used does not detect the VP3 protein (22). As expected, processing of the P1 product by $3C^{pro}$ only resulted in the detection of the VP0 and VP1 products (Fig. 2A, lanes 4, 6, and 8). As expected, the anti-2A antisera detected VP1-2A and/or P1-2A very efficiently from cassettes including P1-2A (Fig. 2B, lanes 3 and 9) but failed to detect products derived from cassettes containing P1 (Fig. 2B, lanes 2, 4, and 6), confirming its specificity for 2A. Note that the free 2A peptide (ca. 2 kDa) was not detected in this immunoblot analysis, since it will have migrated off these gels.

To test whether the VP1/2A cleavage site including the VP1 K210E substitution could be processed by $3C^{pro}$, the P1-2A-mIRES-3C VP1 K210E cDNA cassette encoding this modification was analyzed in the same way. The presence of the K210E substitution within VP1 resulted in a complete block on cleavage of the VP1/2A junction, since VP0 and VP1-2A were produced but not VP1 (Fig. 2A and B, lanes 10). In addition, products corresponding to the processing intermediate VP3-VP1-2A were observed. The mature VP1 protein of serotype O, liberated from the P1 and P1-2A precursors, migrated with higher mobility than the VP1-2A product generated from the wt P1-2A construct and from the VP1 K210E mutant cassette (Fig. 2A and B, lanes 8, 9, and 10).

Using the serotype A cDNA cassettes, the P1 and P1-2A products were again efficiently produced (Fig. 2C, lanes 2 and 3) and were processed by $3C^{pro}$, but only the VP0 and the VP1-2A products were detected by this anti-FMDV antiserum (Fig. 2C, lanes 4 to 9) (note that this antiserum was raised against serotype O FMDV, which may explain its inability to detect the serotype A VP1). Consistent with the results using the type O cassettes, the presence of the K210E substitution in the serotype A VP1 enhanced the level of VP1-2A detected (Fig. 2C and D, lanes 9 and 10) and also resulted in the accumulation of VP3-VP1-2A (Fig. 2C and D, lanes 10). Taken together, these results demonstrated that $3C^{pro}$ was able to process the wt P1-2A precursor at the VP0/VP3, VP3/VP1, and VP1/2A junctions in this expression system but the K210E substitution blocked cleavage of the VP1/2A junction.

Influence of the presence of FMDV 2A peptide on the antigenicity and integrin binding activity of FMDV capsid proteins. The cell lysates used for the immunoblot analyses were also tested using serotype-specific FMDV-antigen ELISAs (Fig. 3A and D)

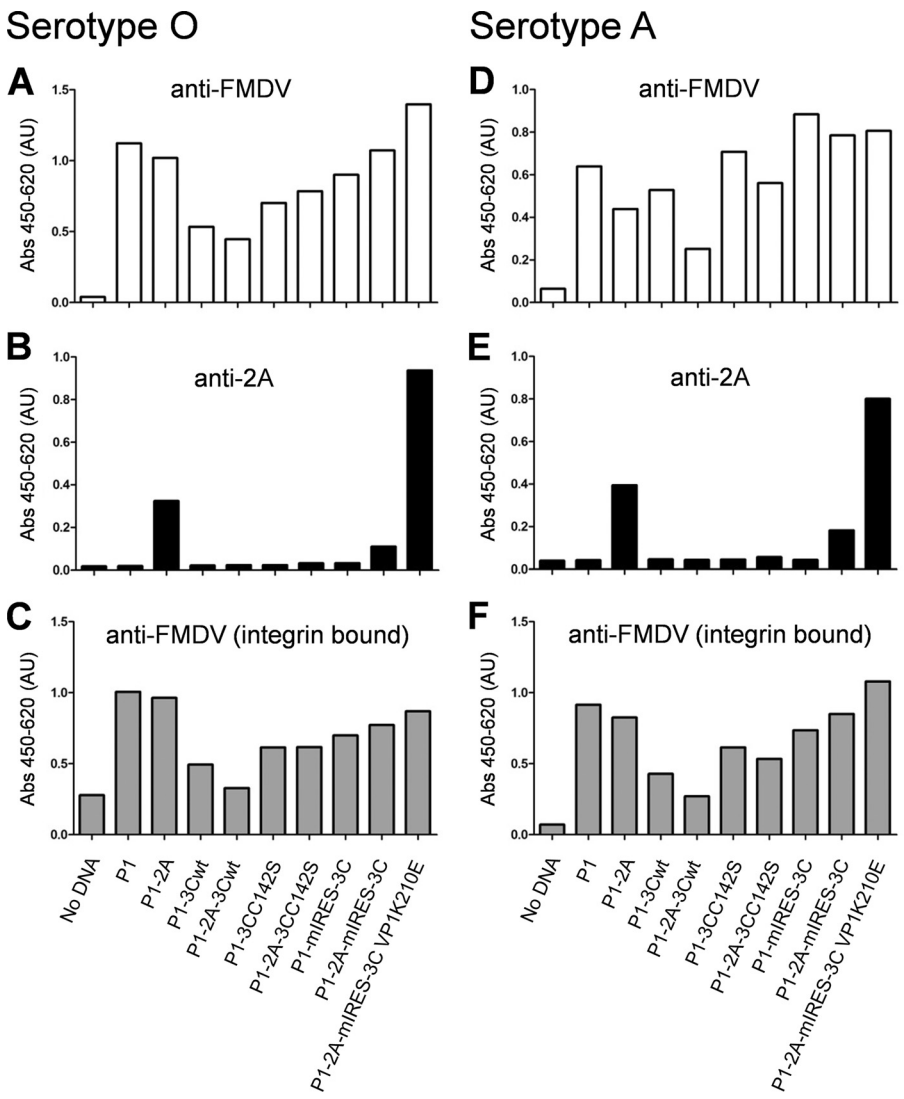

FIG 3 Detection of expressed FMDV capsid proteins using serotype-specific anti-FMDV antibodies and anti-2A antibodies. (A to C) Samples were prepared using serotype O cDNA cassettes as described in the legend to Fig. 2 and analyzed using different anti-FMDV antigen ELISAs as described in Materials and Methods. FMDV proteins captured by rabbit anti-FMDV antibodies were detected directly with guinea pig anti-FMDV antibodies (A), captured with guinea pig anti-FMDV antibodies and detected with anti-2A antibodies (B), or captured by the $\alpha_v\beta_6$ integrin and detected with guinea pig anti-FMDV (C). (D to F) Similarly, samples were prepared using serotype A cDNA cassettes and analyzed using the different FMDV antigen ELISAs in which antibody-captured FMDV proteins were detected directly with anti-FMDV antibodies (D) or with anti-2A antibodies (E) or following capture by the $\alpha_v\beta_6$ integrin and detection with guinea pig anti-FMDV antibodies (F). The results shown are representative of two independent experiments. Samples were analyzed in the same order as described in the legend to Fig. 2. Abs, absorbance; AU, absorbance units.

and an FMDV-2A specific ELISA (Fig. 3B and E). In the serotype-specific FMDV antigen ELISAs (Fig. 3A and D), the unprocessed P1-2A protein, as well as the $3C^{pro}$ processed products derived from it, were efficiently detected using anti-FMDV antibodies, consistent with previous studies (31). Furthermore, very similar results were obtained from these assays with the cassettes that express P1 (Fig. 3A and D). In the ELISAs using the anti-2A antibodies (Fig. 3B and E), polypeptides containing 2A were detected specifically in samples derived from the P1-2A, P1-2A-mIRES-3C, and P1-2A-mIRES-3C VP1 K210E cassettes. It was apparent that the highest signals were observed with products containing the K210E mutant in which the 2A peptide remains fused to VP1. It can be expected that the signal will be higher for the extracts containing the uncleavable VP1-2A than for extracts in which the 2A peptide can be removed, but it is not clear why the signal should be higher than that with extracts containing the unprocessed P1-2A alone. As expected, no signal was detected using this 2A-specfic ELISA in extracts derived from the P1-containing cassettes (Fig. 3B and E). Furthermore, no signal indicative of the presence of 2A was detected from either the P1-2A-3Cwt or P1-2A-3CC142S cassette, consistent with the presence of little or no residual VP1-2A in these samples, as observed in the immunoblots (Fig. 2B and D). As described previously (31), both the unprocessed P1-2A and the fully processed capsid proteins bind to the integrin $\alpha_v\beta_6$ (Fig. 3C and F). By using the P1-mIRES-3C and the P1-2A-mIRES3C VP1 K210E cassettes, it was also shown that neither the absence nor the continued presence of the 2A peptide affected the ability of the capsid proteins to bind to the integrin receptor (Fig. 3C and F).

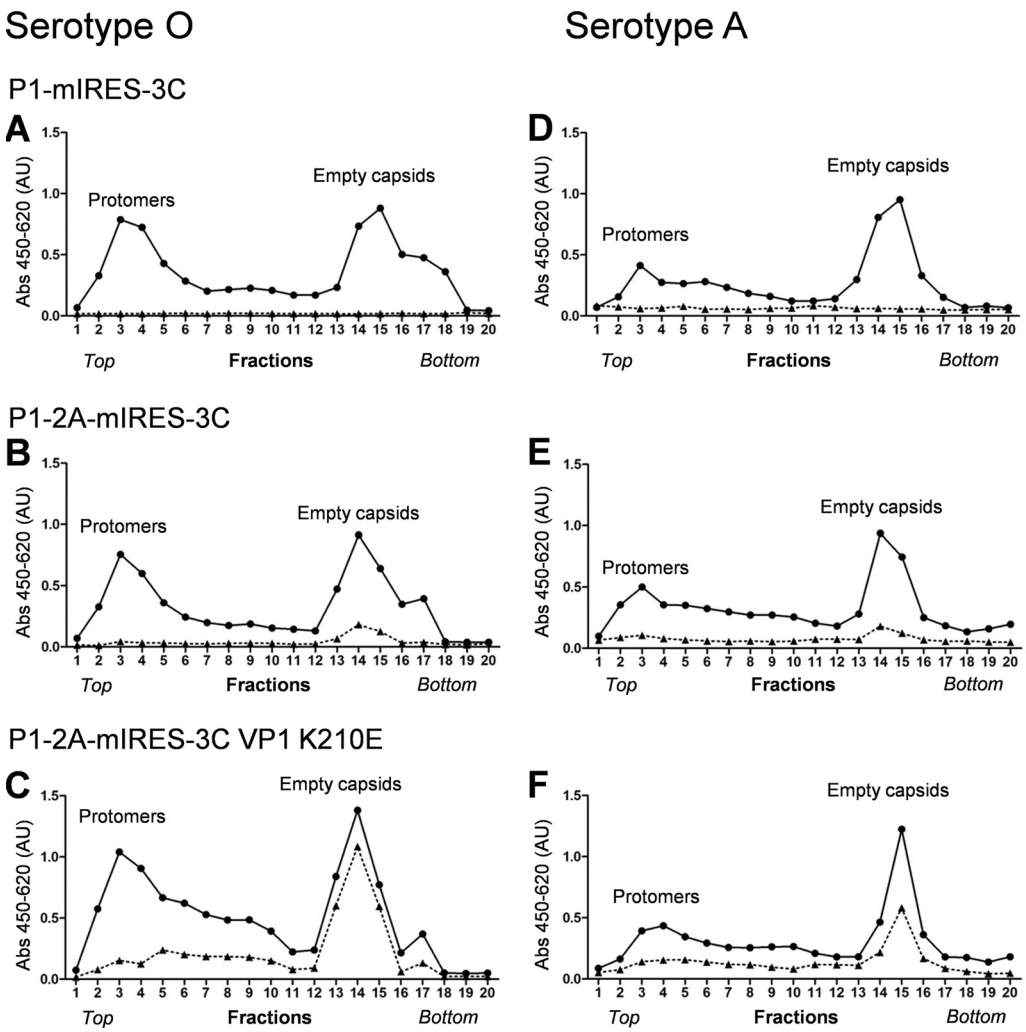

FIG 4 Sucrose gradient profiles of fractionated FMDV protomers and empty capsids formed in cells. BHK cells were transfected as described in the legend to Fig. 2 using the indicated FMDV cDNA cassettes for serotype O (A to C) and serotype A (D to F). Cytoplasmic extracts were prepared 20 h posttransfection and sedimented through gradients of 10 to 30% sucrose. The locations of protomers and empty capsids are indicated. FMDV proteins from each fraction were detected using serotype-specific antigen ELISAs where the antigen was captured on anti-FMDV antibody-coated plates and detected with either serotype-specific guinea pig anti-FMDV antibodies (solid lines) or anti-2A antibodies (dotted lines) as described in Materials and Methods. AU, absorbance units.

Cleavage of the VP1/2A junction is not required for the assembly of empty capsid particles. To determine whether capsid precursors which contained the 2A peptide sequence (due to defective processing of the VP1/2A junction) could form empty capsid particles, proteins expressed from P1-mIRES-3C, P1-2A-mIRES-3C, and P1-2A-mIRES-3C VP1 K210E cDNA cassettes were analyzed by sucrose gradient centrifugation. The fractions were analyzed for the presence of FMDV capsid proteins using FMDV serotype-specific ELISAs and for the presence of the 2A peptide sequence with the 2A ELISA (Fig. 4). As determined by the serotype-specific ELISAs, the major species detected in the fractions were either protomers (Fig. 4, peak at fractions 2 to 4) or empty capsid particles (Fig. 4, peak at fractions 13 to 16). No significant differences in the formation of empty capsid particles, as judged by sedimentation profiles, were observed for the expressed capsid proteins irrespective of whether the cassettes expressed P1-mIRES-3C, P1-2A-mIRES-3C, or P1-2A-mIRES-3C VP1K210E. In extracts from cells transfected with the P1-2A-mIRES-3C cassette, the empty capsid particles (Fig. 4B and E, peak at fractions 13 to 16) contained a low level of VP1-2A, as indicated by the small signal in the 2A-specific ELISA. The presence of the VP1 K210E substitution resulted in a much higher level of 2A reactivity in the empty capsid particle fractions (Fig. 4C and F) without any apparent adverse effect on the formation of the empty capsid particles. Furthermore, the complete absence of the FMDV 2A peptide had no apparent effect on empty capsid formation, since very similar profiles of capsid protein assembly were observed with the P1-mIRES-3C and the P1-2A-mIRES-3C cassettes (Fig. 4A, B, D, and E).

The status of the viral capsid proteins in the initial cell lysates and also in the protomer and empty capsid particle fractions, obtained following sucrose gradient centrifugation, were analyzed by immunoblotting (Fig. 5). The VP1-2A polypeptides were clearly detected (Fig. 5A and B, lanes 7 and 9) both in the cell lysates and in the empty capsid samples (i.e., fraction 14), demonstrating the presence of this novel component within empty capsids and show-

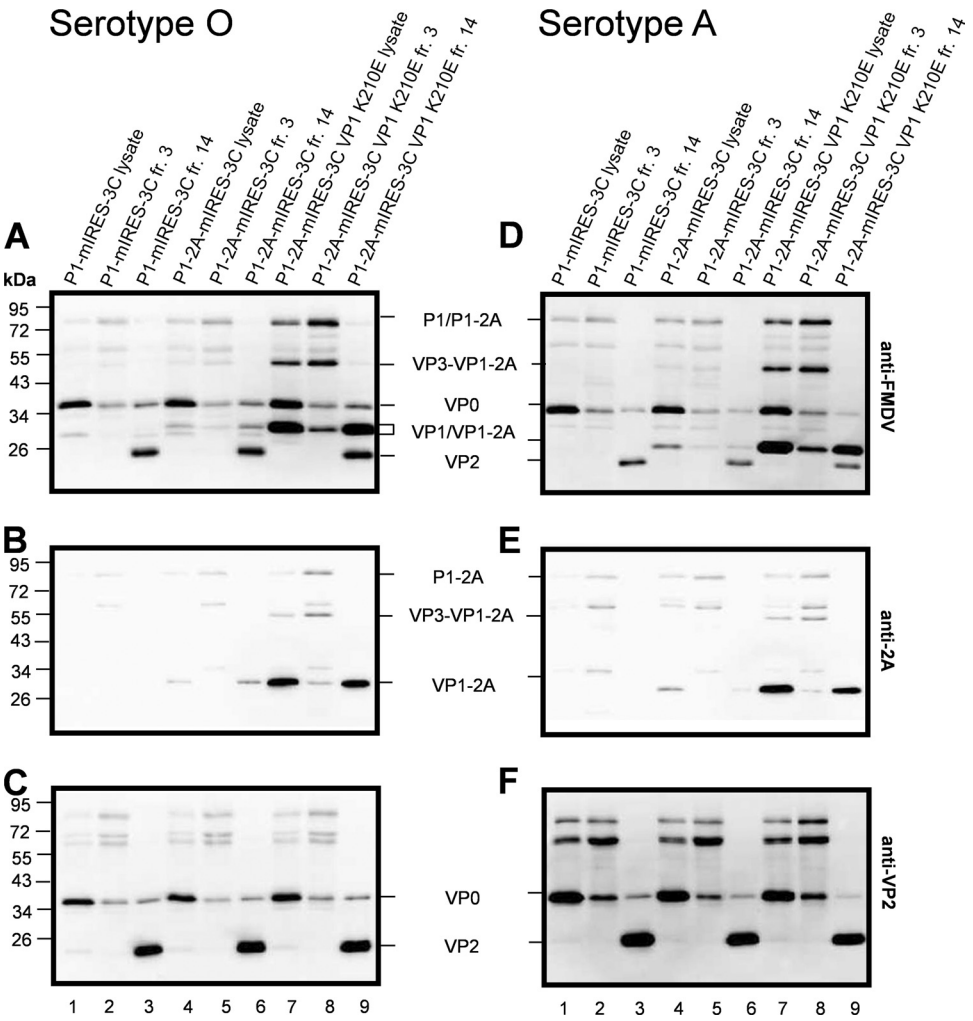

FIG 5 Characterization of FMDV protomers and assembled empty capsids. Aliquots of the whole-cell lysates for serotype O (A to C) and serotype A (D to F), as well as selected fractions containing protomers (fr. 3) and empty capsids (fr. 14), were analyzed by SDS-PAGE and immunoblotting using antibodies specific for FMDV capsid proteins (top), 2A alone (middle), or VP2 alone (bottom). The results shown are representative of two independent experiments. Molecular mass markers (kDa) are indicated in the left margin.

ing that this protein is stable. As reported previously (22, 23), VP0 is readily detected in the initial cell lysates, but during sucrose gradient centrifugation a major proportion of the VP0 in the assembled empty capsid particles is cleaved to generate VP2 (and presumably VP4, although this is not detected in these analyses due to its small size). In contrast, it is interesting that the protomer fractions contained VP0 with little or no VP2 being detected (Fig. 5A and B, lanes 8 and 9); thus, it appears that the VP0 cleavage is dependent on empty capsid assembly.

Influence of S134C and E83K substitutions on capsid assembly. In addition to the K210E change within VP1, which has been clearly shown to modify capsid processing (Fig. 2 and 5), two other substitutions in VP1 were identified within the cell culture-passaged O1 Manisa virus, namely, S134C and E83K (described above). The effects of these substitutions were also examined individually using the P1-2A-mIRES-3C cassettes. The presence of either C134 or S134 in VP1 resulted in the production of protein products which were indistinguishable from each other (Fig. 6A, lanes 2 and 6). However, consistently weaker accumulation of the processed capsid proteins was observed with the E83K mutant (Fig. 6A, lane 3). As described above, the VP1 K210E mutant produced VP1-2A, and significant levels of VP3-VP1-2A also could be seen (Fig. 6A, lane 4). When a double mutant, VP1 E83K and K210E, was analyzed, efficient expression of the same proteins, as observed with the K210E single mutant, was obtained (Fig. 6A, lane 5).

Cell lysates, as analyzed above by immunoblotting, were fractionated using sucrose gradient centrifugation (Fig. 6B to F), and the FMDV capsid proteins and the 2A peptide were detected in the fractions by ELISAs. Clear peaks corresponding to unassembled protomers plus fully assembled empty capsid particles were observed with the wt construct (Fig. 6B), and only a weak signal corresponding to a low level of the 2A peptide (still fused to VP1) was observed in the empty capsid peak (fraction 14). The C134S mutant produced a very similar profile (Fig. 6F). Consistent with the results shown in Fig. 4D, the VP1 K210E mutant yielded similar peaks corresponding to protomers and assembled empty capsids (Fig. 6D), but it also appeared to produce a higher level of

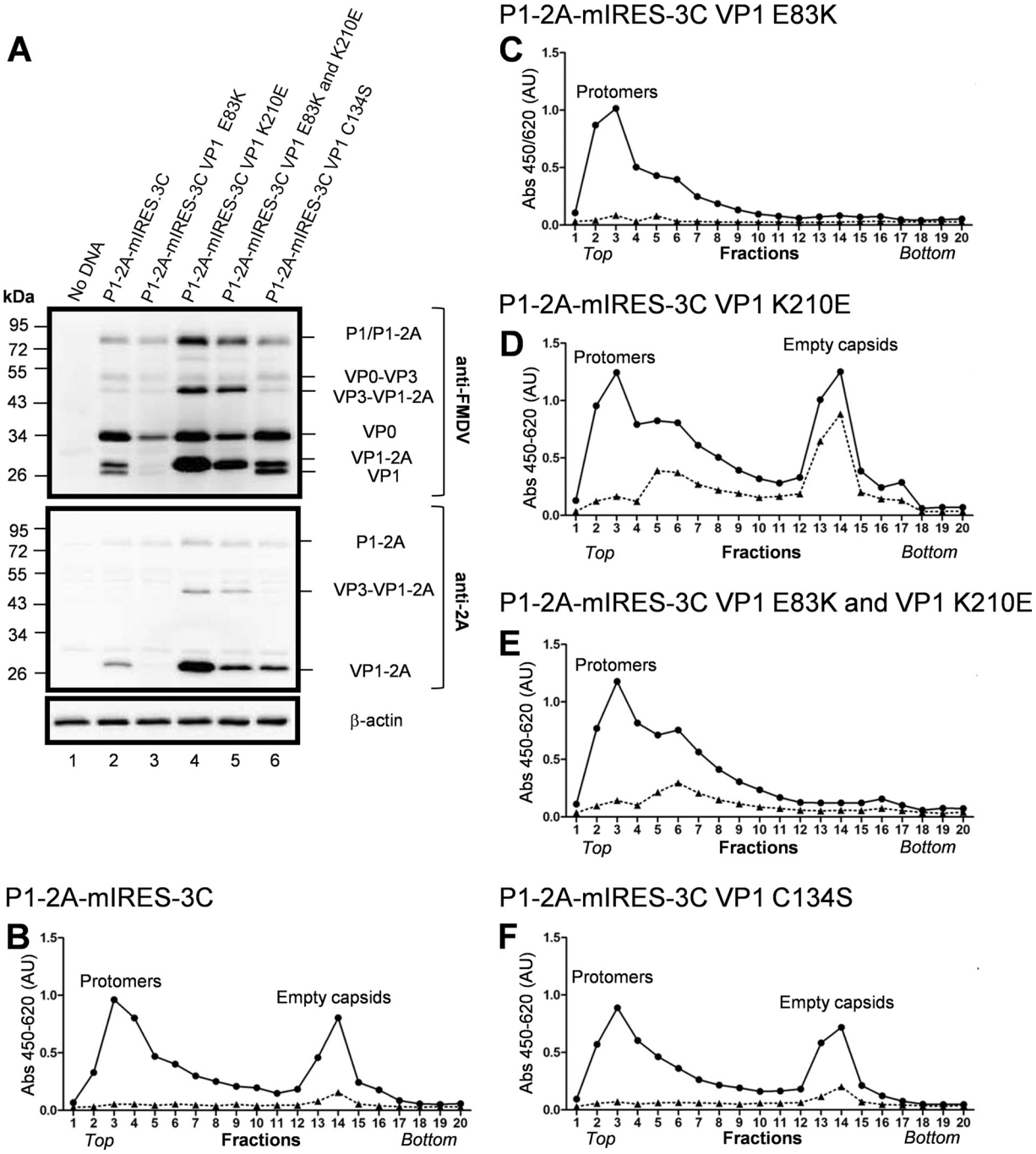

FIG 6 Influence of individual amino acid substitutions within FMDV O1 Manisa VP1 on protein processing and capsid assembly. (A) Cell lysates prepared as described for Fig. 2 using the indicated plasmids were analyzed by immunoblotting using anti-FMDV (top), anti-2A (middle), and anti-β-actin (bottom) antibodies. Molecular mass markers (kDa) are indicated. (B to F) Lysates from cells transfected with the indicated plasmids were also analyzed by sucrose gradient centrifugation. Detection of FMDV proteins (solid lines) and 2A (dotted lines) was achieved by ELISA using anti-FMDV or anti-2A antibodies, respectively, as described for Fig. 3 and 4. Peaks corresponding to the presence of unassembled protomers and empty capsids are labeled. AU, absorbance units.

pentamers (fractions 5 and 6), and a much higher level of 2A was detected in both the pentamer and empty capsid fractions than in the wt construct. In contrast, the E83K mutant generated predominantly protomers (Fig. 6C); however, since the accumulation of FMDV proteins from this construct was less than that from the others (Fig. 6A), we also decided to examine this substitution in the context of the K210E mutation, since the double mutant efficiently produced the expected capsid protein products (Fig. 6A, lane 5). Like the E83K single mutant (and in contrast to the K210E mutant), the E83K K210E double mutant produced only protomers and pentamers with no significant empty capsid peak (Fig. 6E). Thus, it appears that the E83K substitution has a strongly deleterious effect on empty capsid formation. The lack of empty capsid formation was also observed with O1 Manisa (Lindholm) P1-2A,

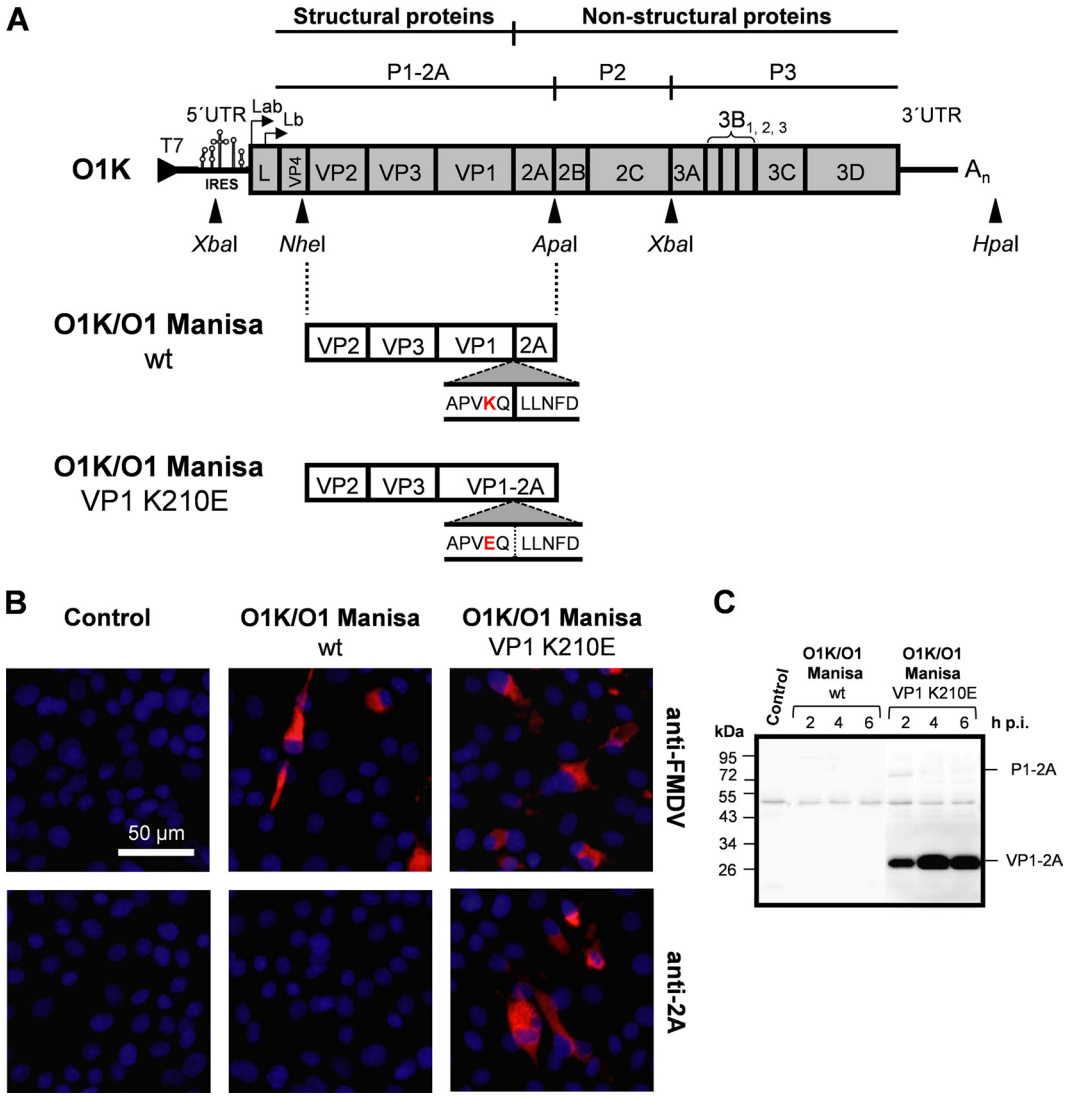

FIG 7 Rescue of infectious FMDV with uncleavable VP1-2A. (A) Schematic representation of the structure of FMDV cDNAs. The structure of the pT7S3 plasmid (39) containing the full-length cDNA of the O1K B64 strain and previously published modifications (40) are shown. The NheI and ApaI restriction enzyme sites (as indicated) were used as described in Materials and Methods to introduce FMDV O1 Manisa wt and VP1 K210E cDNA fragments encoding the capsid proteins VP2-VP3-VP1-2A. The full-length plasmids were linearized using HpaI prior to RNA transcription and electroporation of cells to rescue the viruses. The locations of restriction sites used are indicated: ApaI, HpaI, NheI, and XbaI. (B) Immunostaining of uninfected BHK cells or cells infected (MOI of 0.1) with the rescued FMDV O1K/O1 Manisa wt and VP1 K210E mutant viruses (3rd-passage virus stocks; note that the K210E virus stock has acquired another change, E83K within VP1). FMDV proteins within infected cells were detected (4 h postinfection) with an anti-FMDV O1 Manisa polyclonal antibody or an anti-2A antibody and a secondary antibody labeled with Alexa Fluor 568 (red). The cell nuclei were visualized with DAPI (blue). Bar, 50 μm. (C) Cell lysates were prepared from uninfected BHK cells or from cells infected with the rescued FMDV O1K/O1 Manisa wt and VP1 K210E mutant viruses (at 2, 4, and 6 h postinfection) and analyzed by immunoblotting using anti-2A antibodies. Molecular mass markers (kDa) are indicated.

which contains the three different substitutions together in VP1 (data not shown).

Blocking the cleavage of the VP1/2A junction is tolerated within infectious FMDV. To identify the effect of blocking the VP1/2A cleavage on FMDV infectivity, the mutation required to produce the K210E substitution in VP1 was introduced into a full-length FMDV infectious cDNA clone (Fig. 7A). Chimeric O1K/O1 Manisa cDNAs were prepared that contained the coding sequences for the surface-exposed capsid proteins (VP2, VP3, and VP1) and 2A from O1 Manisa in the backbone of the full-length O1K cDNA (see Materials and Methods). Plasmids containing both the wt O1 Manisa sequence and the mutant with the K210E substitution in VP1 were produced. RNA transcripts were prepared by *in vitro* transcription of the linearized plasmids with T7 RNA polymerase and introduced into BHK cells by electroporation. Viable progeny viruses were recovered from each of the two RNA transcripts and then passaged twice to amplify the virus. The wt and K210E mutant virus stocks (at passage 3) had titers of $10^{7.4}$ and $10^{6.2}$ $TCID_{50}$/ml, respectively. This may indicate that the mutant virus is less fit than the wt virus. Indeed, consistent with this suggestion, rapid reversion of the VP1 K210E substitution has been observed during virus rescue within a serotype A genetic background (data not shown). The sequence of the O1 Manisa capsid coding sequence (VP2-2A) within the rescued viruses was

determined following production of amplicons by reverse transcription-PCR (RT-PCR). The rescued O1K/O1 Manisa wt virus retained the complete O1 Manisa VP2-2A coding sequence in its genome exactly as in the cDNA plasmid after both 2 and 3 passages. Furthermore, the K210E substitution in the VP1/2A junction was retained in the rescued O1K/O1 Manisa VP1 K210E viruses. However, the mutant virus also had acquired a single additional substitution after 3 passages in BHK cells, i.e., an E83K substitution within VP1 which had also been identified in the O1 Manisa (Lindholm) isolate.

To examine the presence of uncleaved VP1-2A within FMDV-infected cells, uninfected and FMDV O1K/O1 Manisa (wt and K210E)-infected BHK cells were stained with both FMDV serotype O-specific and 2A-specific antibodies at 4 h postinfection (Fig. 7B). No staining was detected with either antibody in uninfected cells, as expected. Production of FMDV proteins was detected in cells infected with each of the O1K/O1 Manisa variants. In contrast, the 2A antigen was readily detected within cells infected with the O1K/O1 Manisa VP1 K210E mutant virus in which the VP1/2A junction is modified but not in cells infected with the wt O1K/O1 Manisa virus (Fig. 7B). It seems that the free 2A peptide either is not well recognized by the antisera or, more likely, is rapidly degraded following release from VP1. To confirm the presence of uncleaved VP1-2A in cells infected with the O1K/O1 Manisa VP1 K210E virus, cell extracts prepared at 2, 4, and 6 h postinfection were analyzed by immunoblotting using anti-2A antisera (Fig. 7C). Uncleaved VP1-2A was detected in the samples from cells infected with the K210E mutant virus but not in the samples from cells infected with the O1K/O1 Manisa virus. In similar analyses of cells infected with the O1 Manisa (Lindholm) virus (including the three amino acid substitutions in VP1), the presence of uncleaved VP1-2A has also been demonstrated (data not shown). Thus, these results indicated that VP1/2A cleavage to release the mature VP1 protein is not required for viability of FMDV in cell culture.

DISCUSSION

The specificity of the $3C^{pro}$-mediated processing of the FMDV polyprotein is not completely understood. In contrast to those of many other picornaviruses, FMDV $3C^{pro}$ is able to cleave a variety of different amino acid junctions; these can be grouped into two major classes (26), in which cleavage either occurs at a Q/x or an E/x junction. For these two types of cleavage site, there are particular preferred residues located at specific positions flanking the junction. In the present study, we have examined the processing of the VP1/2A junction ($PxK^{210}Q$/xLNF) and its implications for capsid assembly. The results revealed that a P2-Glu (E) residue at the VP1/2A junction (as in the VP1 K210E mutant) clearly blocked $3C^{pro}$ processing at the modified site, resulting in the persistence of the uncleaved VP1-2A protein. Furthermore, our results also showed that the VP1-2A proteins from two different FMDV serotypes (O and A) are able to assemble, together with VP0 and VP3, into empty capsids, which demonstrates that the C terminus of VP1 clearly tolerates the extension by 2A. However, empty capsid particle formation was also observed after coexpression of the capsid protein precursor completely lacking 2A (i.e., P1) together with $3C^{pro}$ (P1-mIRES-3C). Thus, the presence of 2A is not required for capsid assembly (see the discussion of HAV below), but its presence does not block it. Furthermore, the rescue of infectious FMDV containing uncleavable VP1-2A demonstrates that the presence of the 2A peptide in virus particles can also be tolerated, at least in cell culture. It is interesting that, during passage of the rescued K210E mutant virus, a second site substitution (E83K in VP1) accumulated, and this change had also been observed, in conjunction with the K210E change, in the O1 Manisa (Lindholm) strain. Earlier studies have suggested that the E83K change is a cell culture adaptation in both serotype O and SAT2 viruses (44, 45), which could be consistent with this result. It is noteworthy that the E83K substitution alone or with the K210E change resulted in poor empty capsid formation, but clearly these changes are tolerated within the context of infectious virus. This suggests that the presence of the viral RNA overcomes the instability of the capsid particles induced by the E83K substitution; earlier studies had indicated that the presence of the viral RNA influences the acid stability of FMDV particles (23).

The two intermediate processing products detected in our system, VP3-VP1-2A and VP1-2A, have previously been identified on the basis of partial processing of the P1-2A precursor in rabbit reticulocyte lysate programmed with FMDV O1K transcripts (21). Earlier results suggested a decreased efficiency of cleavage at the VP1/2A junction when $3C^{pro}$ activity is reduced (22, 31), which implies that cleavage at this site is a late event during polyprotein processing of the P1-2A precursor. These data agree with the model proposed previously (29, 48), wherein P1-2A processing by $3C^{pro}$ had the following order of cleavage: VP3/VP1, VP0/VP3, and VP1/2A. Thus, the processing between VP1 and 2A appeared to be the slowest of the $3C^{pro}$-mediated cleavages within the P1-2A precursor. In contrast, the VP1/2A cleavage site was found to be the most rapidly processed protein junction in peptide cleavage assays using short synthetic substrates spanning eight residues on either side of all 10 $3C^{pro}$ cleavage sites (27). However, peptides corresponding to the VP2/VP3, 2C/3A, 3A/3B1, 3B1/3B2, and 3B2/3B3 junctions were uncleaved under these experimental conditions. Recent studies (25) using FMDV capsid precursor proteins and $3C^{pro}$ expressed separately and then incubated together, *in vitro*, produced a different result and suggested that the VP3/VP1 junction was cleaved more slowly than the VP0/VP3 and VP1/2A junctions. The use of transient expression assay systems within mammalian cells, as used here, most closely reflects the environment in which FMDV itself replicates.

It is interesting that blocking the VP1/2A cleavage (as in the VP1 K210E mutant) leads to the detection of the VP3-VP1-2A processing intermediate (Fig. 2A and C, lanes 10). This suggests that the presence of the 2A peptide has adversely affected the rate of VP3/VP1 cleavage, but it is clearly not a complete block, since VP1-2A is also made. It is interesting that in earlier studies (21), it was shown that truncation of P1-2A (removing part of the VP1 sequence) blocked all processing by $3C^{pro}$ *in vitro*.

The results obtained with the K210E mutant confirm that P2-Lys in the VP1/2A junction is an important determinant of $3C^{pro}$ specificity (27, 28). Previously, replacement of P2-Lys by P2-Ala had been shown to abrogate VP1/2A cleavage using a peptide cleavage assay (27). In the same report, P1-Gln replacement with P1-Glu in the VP1/2A site only reduced the cleavage rate. However, curiously, mutation to a P2-Thr residue, a residue found in natural FMDV $3C^{pro}$ substrates (i.e., in the VP3/VP1 junction, also a P1-Gln cleavage site), abrogated cleavage of the VP1/2A peptide substrate (28). It was suggested that Thr is tolerated at P2 in the VP3/VP1 site only together with the particular amino acids present at other positions in the peptide substrate. From the stud-

ies presented here, it appears that the $3C^{pro}$-mediated processing of the VP1/2A junction is tightly constrained and requires a P2-Lys at position 210 of the VP1 protein for two different serotypes. However, it remains to be investigated whether this is generally true (e.g., in other strains or serotypes) or if other modifications can alter this requirement.

For HAV, the VP1-2A polypeptide is found together with VP0 and VP3 in pentamer assemblies (19), and a study of deletion mutants also indicated that the 2A protein participates in the morphogenesis process (18). However, this most likely is not the case for FMDV, since empty capsid particles were also formed using capsid proteins expressed from P1-mIRES-3C cDNA cassettes lacking the 2A protein. Thus, the presence of 2A is not required for the assembly of empty FMDV capsid particles, which is consistent with, but also extends, previous observations which showed that 2A was not required for FMDV pentamer assembly (25).

In the crystal structure of FMDV O1 BFS (43, 46), the C terminus of VP1 is located on the external surface of the virus particle, and residue 211 of VP1 is disordered in the reduced FMDV O1 BFS structure (46). The C-terminal residues (196 to 211) of VP1 form a long arm of surface-exposed residues, and this amino acid sequence traverses the protomer in a clockwise direction, ending near the VP1 GH loop of the 5-fold related protomer. Since the structure is disordered for residue 211 of the VP1 protein (P1-Gln) and the structure with the 2A protein present has not been determined, it is difficult to predict how the presence of the 2A peptide affects the structure. However, based on the results presented here, the presence of the 2A peptide probably causes minimal overall structural disturbance (as described below).

Production of epitope-tagged FMDV particles can allow the development of improved methods for empty capsid and virus purification (e.g., for vaccine production), which can facilitate differentiation between infection and vaccination (DIVA) using the detection of antibodies against the nonstructural proteins which are only induced by infection or vaccination with unpurified vaccines. Previous studies with type C and Asia-1 FMDVs have shown that it is possible to replace and insert peptides into the VP1 GH loop (49, 50). More recently, both FLAG and hemagglutinin (HA) epitope tags have been inserted into the GH loop (between residue 155 and 156) of the VP1 capsid protein and were shown to generate genetically stable infectious FMDVs (51, 52). For the first time, we have now shown that it is possible to produce self-tagged empty capsids for at least two different serotypes of FMDV, these contain no "foreign" sequences but simply retain the 2A peptide. Thus, a single amino acid substitution in the VP1 protein (VP1 K210E) introduces 60 copies of the 2A peptide onto the surface of the icosahedral virus capsid. These empty capsids with the 2A self-tag maintained their structural integrity, and the proteins maintained their ability to bind to the integrin $\alpha_v\beta_6$ (the main FMDV receptor) (Fig. 3C and F). Furthermore, the 2A-tagged capsids also bound to anti-FMDV antibodies and to anti-2A antibodies (Fig. 6D). This fact could be used to facilitate capsid isolation, and one advantage is that this system could be used for empty capsids derived from diverse serotypes of the virus. The maintenance of the usual properties of the empty capsid particles despite the presence of the 2A peptide sequences is fully consistent with the rescue of viable viruses containing this same modification.

Overall, the findings presented here shed further light on features of both the VP1 protein and 2A peptide as a part of the P1-2A precursor, as well as the VP1/2A cleavage site. It is apparent that neither the presence nor the absence of the 2A peptide affects the assembly of FMDV empty capsid particles; indeed, infectious virus can tolerate the presence of uncleaved VP1-2A protein. Thus, this study provides a new strategy to rationally engineer tagged empty capsids and viruses, which could be of importance for future vaccine development.

ACKNOWLEDGMENTS

We thank Li Yu (The Chinese Academy of Agricultural Sciences, China) for the anti-VP2 antibody and Stephen Curry (Imperial College, London, United Kingdom) for useful discussions and the provision of the cleavage site alignments. The excellent technical assistance from Tina Rasmussen, Preben Normann, and Inge Nielsen at Lindholm is also highly appreciated.

This work was supported by the Danish Council for Independent Research–Technology and Production Sciences (FTP grant 09-070549).

REFERENCES

1. **Grubman MJ, Baxt B.** 2004. Foot-and-mouth disease. Clin. Microbiol. Rev. **17:**465–493.
2. **Belsham GJ.** 2005. Translation and replication of FMDV RNA. Curr. Top. Microbiol. Immunol. **288:**43–70.
3. **Fry EE, Stuart DI, Rowlands DJ.** 2005. The structure of foot-and-mouth disease virus. Curr. Top. Microbiol. Immunol. **288:**71–101.
4. **Berryman S, Clark S, Monaghan P, Jackson T.** 2005. Early events in integrin alphavbeta6-mediated cell entry of foot-and-mouth disease virus. J. Virol. **79:**8519–8534.
5. **Martin-Acebes MA, Gonzalez-Magaldi M, Sandvig K, Sobrino F, Armas-Portela R.** 2007. Productive entry of type C foot-and-mouth disease virus into susceptible cultured cells requires clathrin and is dependent on the presence of plasma membrane cholesterol. Virology **369:**105–118.
6. **Johns HL, Berryman S, Monaghan P, Belsham GJ, Jackson T.** 2009. A dominant-negative mutant of rab5 inhibits infection of cells by foot-and-mouth disease virus: implications for virus entry. J. Virol. **83:**6247–6256.
7. **O'Donnell V, LaRocco M, Duque H, Baxt B.** 2005. Analysis of foot-and-mouth disease virus internalization events in cultured cells. J. Virol. **79:**8506–8518.
8. **O'Donnell V, Larocco M, Baxt B.** 2008. Heparan sulfate-binding foot-and-mouth disease virus enters cells via caveola-mediated endocytosis. J. Virol. **82:**9075–9085.
9. **Strebel K, Beck E.** 1986. A second protease of foot-and-mouth disease virus. J. Virol. **58:**893–899.
10. **Hinton TM, Ross-Smith N, Warner S, Belsham GJ, Crabb BS.** 2002. Conservation of L and 3C proteinase activities across distantly related aphthoviruses. J. Gen. Virol. **83:**3111–3121.
11. **Guarne A, Tormo J, Kirchweger R, Pfistermueller D, Fita I, Skern T.** 1998. Structure of the foot-and-mouth disease virus leader protease: a papain-like fold adapted for self-processing and eIF4G recognition. EMBO J. **17:**7469–7479.
12. **Petersen JF, Cherney MM, Liebig HD, Skern T, Kuechler E, James MN.** 1999. The structure of the 2A proteinase from a common cold virus: a proteinase responsible for the shut-off of host-cell protein synthesis. EMBO J. **18:**5463–5475.
13. **Toyoda H, Nicklin MJ, Murray MG, Anderson CW, Dunn JJ, Studier FW, Wimmer E.** 1986. A second virus-encoded proteinase involved in proteolytic processing of poliovirus polyprotein. Cell **45:**761–770.
14. **Donnelly ML, Luke G, Mehrotra A, Li X, Hughes LE, Gani D, Ryan MD.** 2001. Analysis of the aphthovirus 2A/2B polyprotein "cleavage" mechanism indicates not a proteolytic reaction, but a novel translational effect: a putative ribosomal "skip." J. Gen. Virol. **82:**1013–1025.
15. **Martin A, Benichou D, Chao SF, Cohen LM, Lemon SM.** 1999. Maturation of the hepatitis A virus capsid protein VP1 is not dependent on processing by the 3Cpro proteinase. J. Virol. **73:**6220–6227.
16. **Probst C, Jecht M, Gauss-Muller V.** 1999. Intrinsic signals for the assembly of hepatitis A virus particles. Role of structural proteins VP4 and 2A. J. Biol. Chem. **274:**4527–4531.
17. **Rachow A, Gauss-Muller V, Probst C.** 2003. Homogeneous hepatitis A virus particles. Proteolytic release of the assembly signal 2A from procapsids by factor Xa. J. Biol. Chem. **278:**29744–29751.

18. **Cohen L, Benichou D, Martin A.** 2002. Analysis of deletion mutants indicates that the 2A polypeptide of hepatitis A virus participates in virion morphogenesis. J. Virol. **76:**7495–7505.
19. **Borovec SV, Anderson DA.** 1993. Synthesis and assembly of hepatitis A virus-specific proteins in BS-C-1 cells. J. Virol. **67:**3095–3102.
20. **Donnelly ML, Hughes LE, Luke G, Mendoza H, ten Dam E, Gani D, Ryan MD.** 2001. The "cleavage" activities of foot-and-mouth disease virus 2A site-directed mutants and naturally occurring "2A-like" sequences. J. Gen. Virol. **82:**1027–1041.
21. **Ryan MD, Belsham GJ, King AM.** 1989. Specificity of enzyme-substrate interactions in foot-and-mouth disease virus polyprotein processing. Virology **173:**35–45.
22. **Gullberg M, Muszynzki B, Organtini LJ, Ashley RE, Hafenstein SL, Belsham GJ, Polacek C.** 2013. Assembly and characterization of foot-and-mouth disease virus empty capsid particles expressed within mammalian cells. J. Gen. Virol. **94:**1769–1779.
23. **Curry S, Abrams CC, Fry E, Crowther JC, Belsham GJ, Stuart DI, King AM.** 1995. Viral RNA modulates the acid sensitivity of foot-and-mouth disease virus capsids. J. Virol. **69:**430–438.
24. **Porta C, Kotecha A, Burman A, Jackson T, Ren J, Loureiro S, Jones IM, Fry EE, Stuart DI, Charleston B.** 2013. Rational engineering of recombinant picornavirus capsids to produce safe, protective vaccine antigen. PLoS Pathog. **9:**e1003255. doi:10.1371/journal.ppat.1003255.
25. **Goodwin S, Tuthill TJ, Arias A, Killington RA, Rowlands DJ.** 2009. Foot-and-mouth disease virus assembly: processing of recombinant capsid precursor by exogenous protease induces self-assembly of pentamers in vitro in a myristoylation-dependent manner. J. Virol. **83:**11275–11282.
26. **Curry S, Roque-Rosell N, Zunszain PA, Leatherbarrow RJ.** 2007. Foot-and-mouth disease virus 3C protease: recent structural and functional insights into an antiviral target. Int. J. Biochem. Cell Biol. **39:**1–6.
27. **Birtley JR, Knox SR, Jaulent AM, Brick P, Leatherbarrow RJ, Curry S.** 2005. Crystal structure of foot-and-mouth disease virus 3C protease. New insights into catalytic mechanism and cleavage specificity. J. Biol. Chem. **280:**11520–11527.
28. **Zunszain PA, Knox SR, Sweeney TR, Yang J, Roque-Rosell N, Belsham GJ, Leatherbarrow RJ, Curry S.** 2010. Insights into cleavage specificity from the crystal structure of foot-and-mouth disease virus 3C protease complexed with a peptide substrate. J. Mol. Biol. **395:**375–389.
29. **Bablanian GM, Grubman MJ.** 1993. Characterization of the foot-and-mouth disease virus 3C protease expressed in Escherichia coli. Virology **197:**320–327.
30. **Belsham GJ, Brangwyn JK, Ryan MD, Abrams CC, King AM.** 1990. Intracellular expression and processing of foot-and-mouth disease virus capsid precursors using vaccinia virus vectors: influence of the L protease. Virology **176:**524–530.
31. **Polacek C, Gullberg M, Li J, Belsham GJ.** 2013. Low levels of foot-and-mouth disease virus $3C^{pro}$ expression are required to achieve optimal capsid protein expression and processing in mammalian cells. J. Gen. Virol. **94:**1249–1258.
32. **Sambrook J, Fritsch EF, Maniatis T.** 1989. Molecular cloning: a laboratory manual, 2nd ed. Cold Spring Harbor Laboratory Press, Cold Spring Harbor, NY.
33. **Fuerst TR, Niles EG, Studier FW, Moss B.** 1986. Eukaryotic transient-expression system based on recombinant vaccinia virus that synthesizes bacteriophage T7 RNA polymerase. Proc. Natl. Acad. Sci. U. S. A. **83:**8122–8126.
34. **Belsham GJ, Nielsen I, Normann P, Royall E, Roberts LO.** 2008. Monocistronic mRNAs containing defective hepatitis C virus-like picornavirus internal ribosome entry site elements in their 5′ untranslated regions are efficiently translated in cells by a cap-dependent mechanism. RNA **14:**1671–1680.
35. **Yu Y, Wang H, Zhao L, Zhang C, Jiang Z, Yu L.** 2011. Fine mapping of a foot-and-mouth disease virus epitope recognized by serotype-independent monoclonal antibody 4B2. J. Microbiol. **49:**94–101.
36. **Roeder PL, Le Blanc Smith PM.** 1987. Detection and typing of foot-and-mouth disease virus by enzyme-linked immunosorbent assay: a sensitive, rapid and reliable technique for primary diagnosis. Res. Vet. Sci. **43:**225–232.
37. **OIE.** 2009. Foot-and-mouth disease. Manual of standards for diagnostic test and vaccines for terrestrial animals. World Organization for Animal Health (OIE), Paris, France. http://web.oie.int/eng/normes/MMANUAL/A_Index.htm.
38. **Ferris NP, Abrescia NG, Stuart DI, Jackson T, Burman A, King DP, Paton DJ.** 2005. Utility of recombinant integrin alpha v beta6 as a capture reagent in immunoassays for the diagnosis of foot-and-mouth disease. J. Virol. Methods **127:**69–79.
39. **Ellard FM, Drew J, Blakemore WE, Stuart DI, King AM.** 1999. Evidence for the role of His-142 of protein 1C in the acid-induced disassembly of foot-and-mouth disease virus capsids. J. Gen. Virol. **80:**1911–1918.
40. **Bøtner A, Kakker NK, Barbezange C, Berryman S, Jackson T, Belsham GJ.** 2011. Capsid proteins from field strains of foot-and-mouth disease virus confer a pathogenic phenotype in cattle on an attenuated, cell-culture-adapted virus, O1 Kaufbeuren virus. J. Gen. Virol. **92:**1141–1151.
41. **Nayak A, Goodfellow IG, Woolaway KE, Birtley J, Curry S, Belsham GJ.** 2006. Role of RNA structure and RNA binding activity of foot-and-mouth disease virus 3C protein in VPg uridylylation and virus replication. J. Virol. **80:**9865–9875.
42. **Reed LJ, Muench H.** 1938. A simple method of estimating fifty percent endpoints. Am. J. Hyg. **27:**493–497.
43. **Acharya R, Fry E, Stuart D, Fox G, Rowlands D, Brown F.** 1989. The three-dimensional structure of foot-and-mouth disease virus at 2.9 A resolution. Nature **337:**709–716.
44. **Zhao Q, Pacheco JM, Mason PW.** 2003. Evaluation of genetically engineered derivatives of a Chinese strain of foot-and-mouth disease virus reveals a novel cell-binding site which functions in cell culture and in animals. J. Virol. **77:**3269–3280.
45. **Maree FF, Blignaut B, de Beer TA, Visser N, Rieder EA.** 2010. Mapping of amino acid residues responsible for adhesion of cell culture-adapted foot-and-mouth disease SAT type viruses. Virus Res. **153:**82–91.
46. **Logan D, Abu-Ghazaleh R, Blakemore W, Curry S, Jackson T, King A, Lea S, Lewis R, Newman J, Parry N, Rowlands D, Stuart D, Fry E.** 1993. Structure of a major immunogenic site on foot-and-mouth disease virus. Nature **362:**566–568.
47. **Carrillo C, Tulman ER, Delhon G, Lu Z, Carreno A, Vagnozzi A, Kutish GF, Rock DL.** 2005. Comparative genomics of foot-and-mouth disease virus. J. Virol. **79:**6487–6504.
48. **Grubman MJ, Zellner M, Bablanian G, Mason PW, Piccone ME.** 1995. Identification of the active-site residues of the 3C proteinase of foot-and-mouth disease virus. Virology **213:**581–589.
49. **Baranowski E, Ruiz-Jarabo CM, Lim F, Domingo E.** 2001. Foot-and-mouth disease virus lacking the VP1 G-H loop: the mutant spectrum uncovers interactions among antigenic sites for fitness gain. Virology **288:**192–202.
50. **Wang H, Xue M, Yang D, Zhou G, Wu D, Yu L.** 2012. Insertion of type O-conserved neutralizing epitope into the foot-and-mouth disease virus type Asia1 VP1 G-H loop: effect on viral replication and neutralization phenotype. J. Gen. Virol. **93:**1442–1448.
51. **Seago J, Jackson T, Doel C, Fry E, Stuart D, Harmsen MM, Charleston B, Juleff N.** 2012. Characterization of epitope-tagged foot-and-mouth disease virus. J. Gen. Virol. **93:**2371–2381.
52. **Lawrence P, Pacheco JM, Uddowla S, Hollister J, Kotecha A, Fry E, Rieder E.** 2013. Foot-and-mouth disease virus (FMDV) with a stable FLAG epitope in the VP1 G-H loop as a new tool for studying FMDV pathogenesis. Virology **436:**150–161.